Life Sciences 235 (2019) 116863

Contents lists available at ScienceDirect

Life Sciences

journal homepage: www.elsevier.com/locate/lifescie

Dimethyl fumarate attenuates lipopolysaccharide-induced mitochondrial injury by activating Nrf2 pathway in cardiomyocytes

Chun-Yan Fu[a], Jun Chen[a], Xiao-Yang Lu[a], Ming-Zhi Zheng[b], Lin-Lin Wang[c], Yue-Liang Shen[a,*], Ying-Ying Chen[a,*]

[a] Department of Pathology and Pathophysiology, Zhejiang University School of Medicine, Hangzhou 310058, China
[b] Department of Pharmacology, Hangzhou Medical College, Hangzhou 310053, China
[c] Center for Stem Cell and Tissue Engineering, Zhejiang University School of Medicine, Hangzhou 310058, China

ARTICLE INFO

Keywords:
Dimethyl fumarate
Lipopolysaccharide
Nrf2
Mitochondria

ABSTRACT

Aims: To determine whether dimethyl fumarate (DMF) can protect against lipopolysaccharide (LPS) -induced myocardial injury.

Main methods: H9c2 cells pretreated with or without DMF were stimulated with LPS. Cell viability and apoptosis were evaluated. Nrf2 and HO-1 expression were detected using Western blotting. Mitochondrial morphology, mitochondrial superoxide production were observed using confocal microscope. Mitochondrial respiration function was measured using Seahorse bioanalyzer.

Key findings: (1) The cell viability decreased, LDH release and apoptosis increased in LPS- challenged H9c2 cells. DMF pretreatment brought a higher cell viability, and a lower LDH leakage and apoptosis than those of LPS group ($P < 0.01$). (2) DMF pretreatment resulted in an increased Nrf2 and HO-1 expression, and enhanced nuclear Nrf2 level in LPS-challenged cells ($P < 0.01$). (3) Nrf2-siRNA could inhibit DMF-induced enhancement of HO-1 expression and cell viability, and partly abolish DMF-induced reduction of LDH leakage and apoptosis. (4) ERK1/2 inhibitor PD98059 could not only prevent the DMF-induced enhancement of nuclear Nrf2 and HO-1, but also inhibit DMF-induced increase in cell viability. (5) Compared with LPS-challenged cells, DMF pretreatment caused a lower production of mitochondrial superoxide and a higher mitochondrial membrane potential, which could be abolished by Nrf2-siRNA. (6) DMF could attenuate LPS-induced mitochondrial fragmentation and improve mitochondrial respiration function by enhancement of the oxygen consumption rate of basal respiration and ATP production in LPS-challenged cells ($P < 0.01$).

Significance: DMF protects cardiomyocytes against LPS-induced damage. ERK1/2-dependent activation of Nrf2/HO-1 pathway is responsible for DMF-induced cardioprotection *via* reduction of oxidative stress, improvement of mitochondrial morphology and energy metabolism.

1. Introduction

Sepsis is a life-threatening disorder of systemic inflammatory response syndrome, and most septic patients could progress to multiple organ failure [1]. Myocardial impairment is a common clinical feature of severe sepsis [2]. The mortality of septic patients with cardiac dysfunction is approximately 70%, which is much higher than those without cardiac dysfunction [3]. Many studies demonstrated that cardiac oxidative damage, mitochondrial dysfunction and bioenergetics processes impairment are the basic pathophysiological mechanisms of myocardial dysfunction during sepsis [4,5]. However, effective therapeutic strategies to prevent sepsis-induced cardiac dysfunction are still not yet established.

Dimethyl fumarate (DMF) is a fumaric acid, which can mainly be hydrolyzed by esterase into monomethyl fumarate [6]. DMF and its metabolite monomethyl fumarate exert pharmacological effects in many pathological conditions. DMF could alleviate oxidative stress-induced damage and apoptosis in 7-ketocholesterol-treated oligoden-

* Corresponding authors at: Department of Pathology and Pathophysiology, Zhejiang University School of Medicine, 866 Yuhangtang Road, Hangzhou 310058, China.
E-mail addresses: shenyueliang@zju.edu.cn (Y.-L. Shen), bchenyy@zju.edu.cn (Y.-Y. Chen).

https://doi.org/10.1016/j.lfs.2019.116863
Received 18 July 2019; Received in revised form 2 September 2019; Accepted 9 September 2019
Available online 09 September 2019
0024-3205/

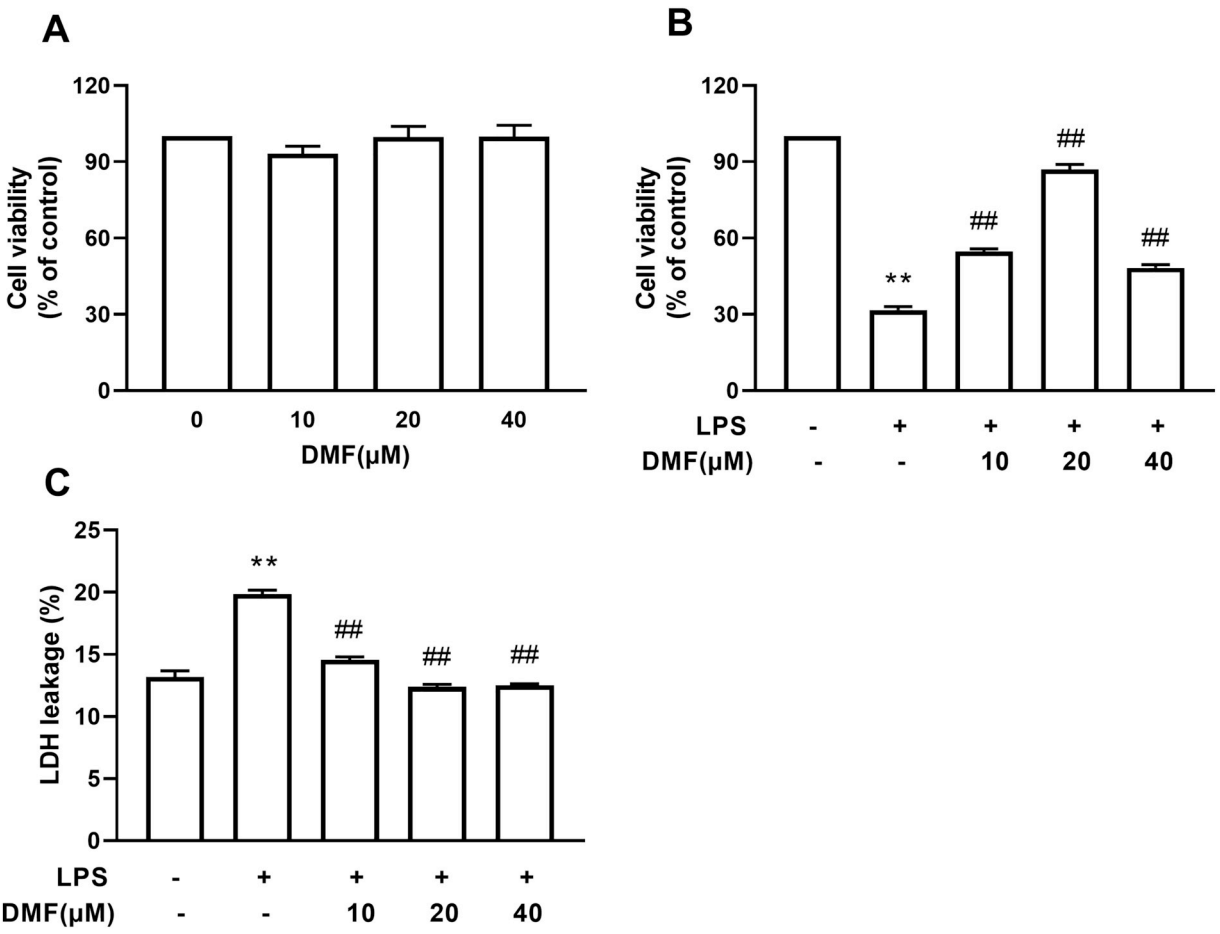

Fig. 1. Effect of DMF on LPS-induced cell injury in H9c2 cells. (A-B) Cell viability measured using CCK-8 assay. (C) LDH leakage. Data were expressed as mean ± SEM ($n = 6$). $^{**}P < 0.01$ *vs* control group; $^{\#\#}P < 0.01$ *vs* LPS group.

drocytes [7]. DMF reduces brain edema and improves neurobehavioral function in acute cerebral ischemia mice by increasing the expression of antioxidant proteins and blocking glutamate-induced neuronal excitotoxicity [8,9]. In isoproterenol-induced cardiac hypertrophy model, DMF was proven to exert cardioprotective effect though interfering with MyD88-dependent toll-like receptor signaling pathway [10]. Since DMF possesses anti-inflammatory and anti-oxidative characteristics in various tissues, we hypothesize that it might also protect against sepsis-induced myocardial dysfunction.

Transcription factor nuclear factor erythroid 2 related factor (Nrf2) is an important protein in protecting cells against oxidative stress injury [11]. In many pathological conditions such as atherosclerosis and ischemia-reperfusion, Nrf2 has been demonstrated to have a potential cardiac protective characteristics [12]. Studies have also shown that neuroprotective effect of DMF is mediated by an Nrf2-dependent mechanism [8,9]. Whether Nrf2 is also an important mediator in the cardioprotection of DMF against sepsis-induced cardiac damage is still unclear.

The objectives of present study were to investigate whether DMF can protect against lipopolysaccharide (LPS)-induced cardiomyocytes damage, and to further explore whether Nrf2 pathway participates in the myocardial beneficial effect of DMF.

2. Materials and methods

2.1. Reagents

DMF and LPS were from Merck KGaA (Darmstadt, Germany). PD98059 was obtained from Selleck chemicals (Houston, TX, USA). Dulbecco's modified Eagle's medium (DMEM) was from GIBCO Laboratories (Grand Island, NY, USA). Antibody against Nrf2 was purchased from Abcam (Cambridge, UK). Antibodies against HO-1, p-Erk1/2, Erk1/2 and Lamin A/C were from Cell Signaling (Danvers, MA, USA). GAPDH antibody was from EarthOx Life Sciences (Millbrae, CA, USA). JC-1 dye was from Beyotime (Shanghai, China). Nuclear and cytoplasmic extraction regents, protease and phosphatase inhibitor cocktail, Mito-Tracker Deep Red, MitoSOX Red, and rat IL-1β ELISA kit were purchased from Affymetrix eBioscience (San Diego, CA, USA). Cell counting kit-8 (CCK-8) was from Dojindo (Kyushu, Japan). Rat IL-18 ELISA kit was from Rockland (Pottstown, PA, USA).

2.2. Cell culture

H9c2 cells were obtained from Chinese Academy of Sciences (Shanghai, China). The cells were cultured in DMEM containing 10%

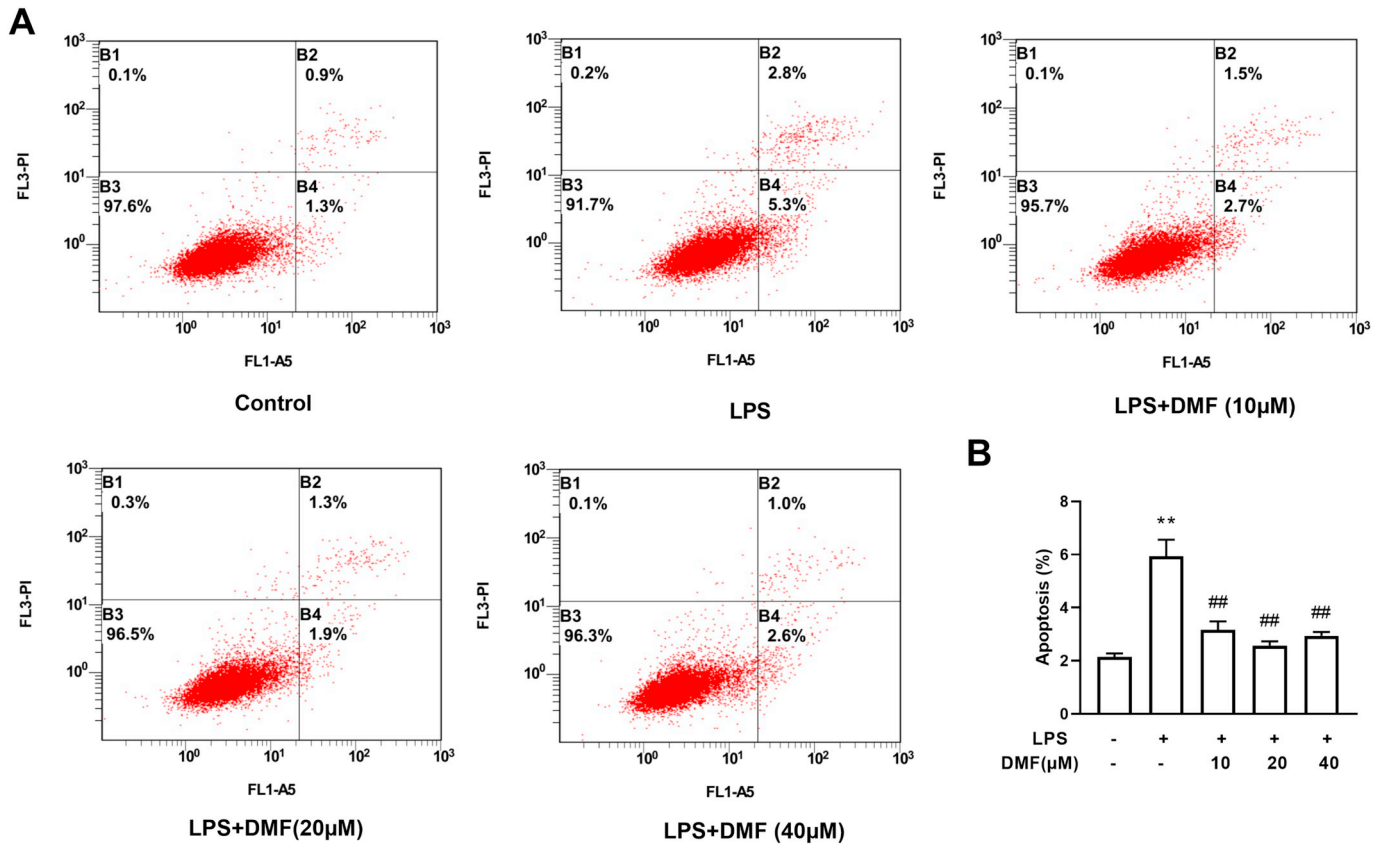

Fig. 2. Effect of DMF on LPS-induced apoptosis in H9c2 cells. (A) Representative flow cytometry results obtained with Annexin V-FITC (A5) and propidium iodide (PI). (B) Data analysis showing apoptosis. Data were expressed as mean ± SEM ($n = 6$). $^{**}P < 0.01$ *vs* control group; $^{\#\#}P < 0.01$ *vs* LPS group.

FBS. All cells were maintained at 37 °C and an atmosphere of 5% CO_2. Two hours before exposure to LPS (1.0 μg/ml), cells were incubated with or without DMF (10, 20, 40 μM). After treatment with LPS for 6 h, expression and location of target proteins were detected. Other parameters were all evaluated after 24 h exposure to LPS.

2.3. Evaluation of cell viability

After treatments, cells were cultured in medium containing 10% CCK-8 for 60 min. Optical density at 450 nm was measured using a microplate reader (Bio-Rad, Hercules, CA).

2.4. LDH activity assay

After different pretreatments, the culture supernatant was collected and cells were lysed. Lactate dehydrogenase (LDH) activity was detected using LDH detection kit (Beyotime, Shanghai, China), and evaluated at 490 nm by a microplate reader. Percentage of LDH leakage from cell was calculated by dividing LDH in culture media by total LDH (media plus lysate).

2.5. Flow cytometry analysis of apoptosis

Cell apoptosis was detected using Annexin V/PI apoptosis kit (Multi Sciences Biotech, Hangzhou, China). Briefly, after various treatments, cells were stained with 5 μl Annexin V-FITC in 500 μl staining buffer for 10 min. After that 10 μl propidium iodide (PI) was added and cells were continuously incubated for 5 min at room temperature, and protected from light. The number of apoptotic cells was evaluated using a flow cytometry (Beckman Coulter, USA).

2.6. Western blotting

Total cellular protein was obtained by lysing cells with cell lysis buffer including protease and phosphatase inhibitor cocktail and 1% PMSF. Cytosolic and nuclear proteins of H9c2 cells were separated by using commercial Kit. Protein concentration was determined by bicinchoninic acid assay. Proteins were separated based on their mass using 10% or 12% SDS-PAGE. The separated protein was then blotted onto nitrocellulose membranes in transfer buffer at 200 mV. After blocked, nitrocellulose membranes were incubated overnight at 4 °C with antibodies against Nrf2 (1:2000), HO-1 (1:1000), p-ERK1/2 (1:2000), ERK1/2 (1:1000), Lamin A/C (1:2000), or glyceraldehyde 3-phosphate dehydrogenase (GAPDH, 1:5000). After washed with TBST, blots were incubated with near-infrared-labeled secondary antibodies (Li-COR Biosciences, Lincoln, NE, USA) for 60 min. Protein band signals were detected using Odyssey CLx Near-Infrared Imaging System (Li-COR Biosciences, Lincoln, NE, USA).

2.7. Location of Nrf2 assay

Location of Nrf2 protein was analyzed using immunofluorescence

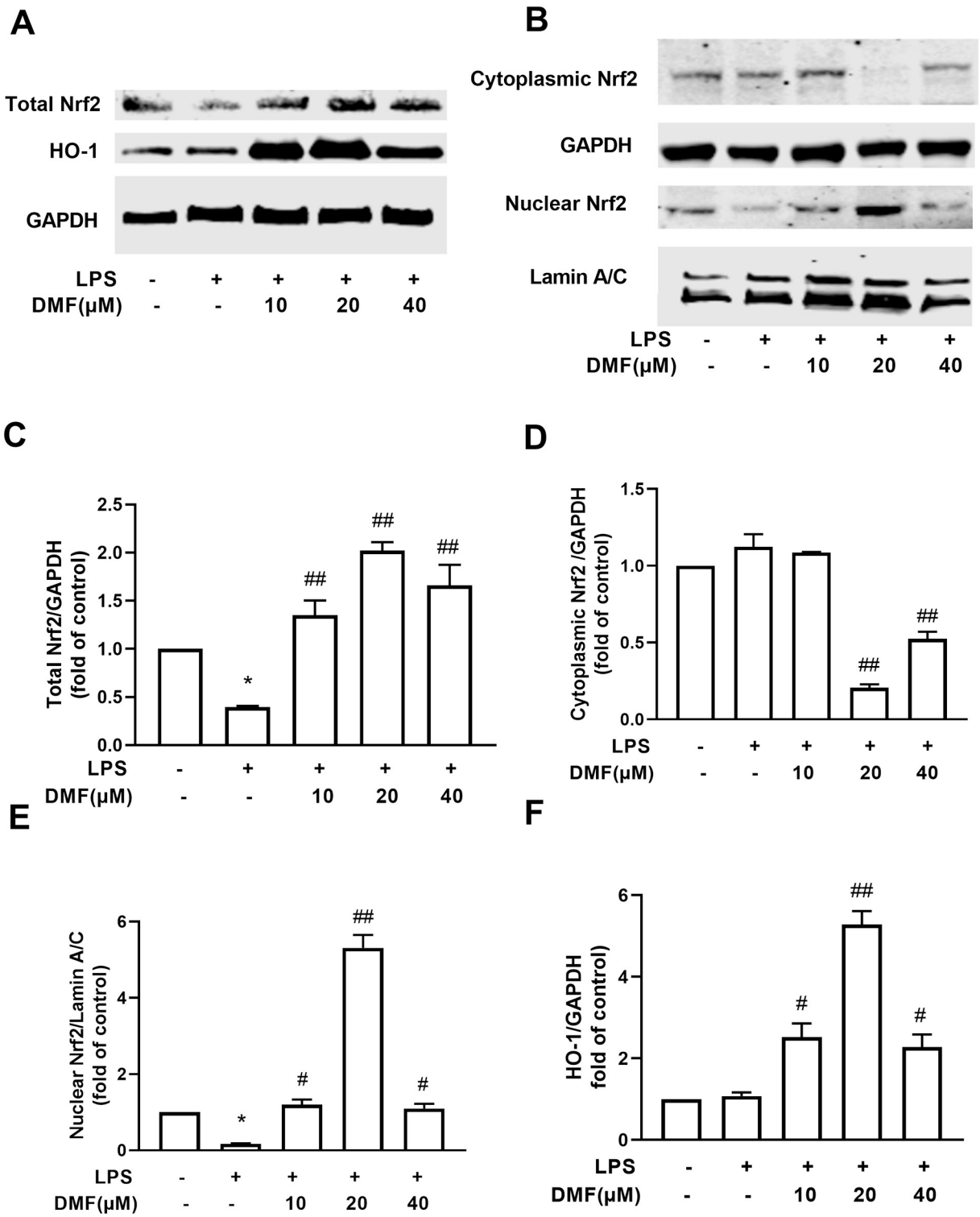

Fig. 3. Effect of DMF on Nrf2/HO-1 signaling in LPS-challenged H9c2 cells. (A, B) Representative immunoblot obtained with HO-1, Nrf2, GAPDH and Lamin A/C antibodies. (C– F) Densitometric analysis showing the expression of HO-1 and Nrf2 protein. GAPDH and Lamin A/C were served as cytoplasmic or nuclear internal controls, respectively. Data are mean ± SEM ($n = 3$). $^{*}P < 0.05$ *vs* control group; $^{\#}P < 0.05$, $^{\#\#}P < 0.01$ *vs* LPS group. (G) Location of Nrf2 protein (green) was detected using immunofluorescence assays. Scale bars = 20 μm. (For interpretation of the references to color in this figure legend, the reader is referred to the web version of this article.)

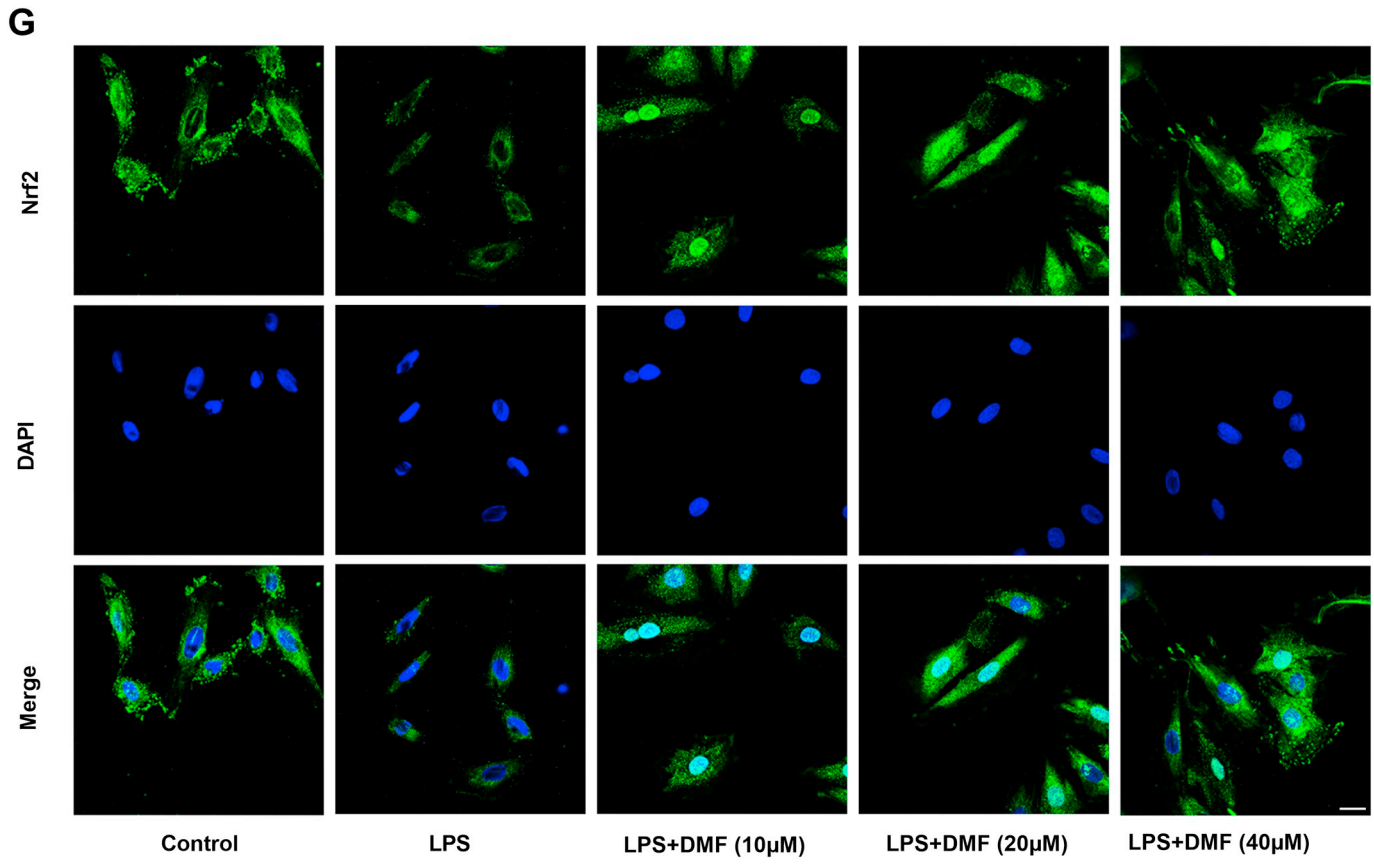

Fig. 3. (*continued*)

technique. H9c2 cells were first kept in 4% paraformaldehyde for 15 min. Then cells were permeabilized with 1% Triton X-100 for 15 min, and blocked in blocking buffer for 30 min. Cells were maintained in Nrf2 antibody (1: 50) for 12 h at 4 °C, Cy3-conjugated IgG (1: 200) for 2 h, and finally stained with DAPI. Images were obtained using a confocal microscope.

2.8. Transfection of Nrf2-siRNA

siRNAs were synthesized by GenePharma (Shanghai, China). Cells were allowed to reach 60% confluence. Then 20 nM of Nrf2-siRNA or control siRNA was transfected into H9c2 cells using Lipofectamine 3000 reagent (Affymetrix eBioscience, San Diego, CA, US). The transfection efficiency was analyzed using PCR method. siRNA sequences used in this study are as follows:

SiRNA1	sense: CCCUGUGUAAAGCUUUCAATT anti-sense: GAAAGCUUUACACAGGGTT
SiRNA2	sense: GUCAGCGACAGAAGGAUUATT anti-sense: AUCCUUCUGUCGCUGACTT
Negative control siRNA	sense: UUCUCCGAACGUGUCACGUTT anti-sense: ACGUGACACGUUCGGAGAATT

2.9. Measurement of IL-1β and IL-18

The culture medium of H9c2 cells was collected. Concentration of IL-1β and IL-18 in supernatant was measured using ELISA kits. The absorbance at 450 nm was detected by a microplate reader.

2.10. Determination of MDA content, GSH level, SOD and GSH-Px activities

After various treatments, cells were lysed and cell lysates were collected. Then malondialdehyde (MDA) content, glutathione (GSH) level, superoxide dismutase (SOD) and glutathione peroxidase (GSH-Px) activities were quantitative analyzed using relevant commercial kits (Beyotime, Shanghai, China). MDA, GSH, SOD and GSH-Px activities were determined by measuring the absorbance in wavelength of 532 nm, 412 nm, 450 nm and 340 nm, respectively.

2.11. Mitochondrial superoxide production assay

After treatments, culture medium was removed and cells were loaded with 2.5 μM MitoSOX Red for 30 min at 37 °C. Cells were observed under a microscope with Ex 510 nm/Em 580 nm (Olympus, Tokyo, Japan). Mitochondrial superoxide production was calculated by measuring red fluorescence intensity.

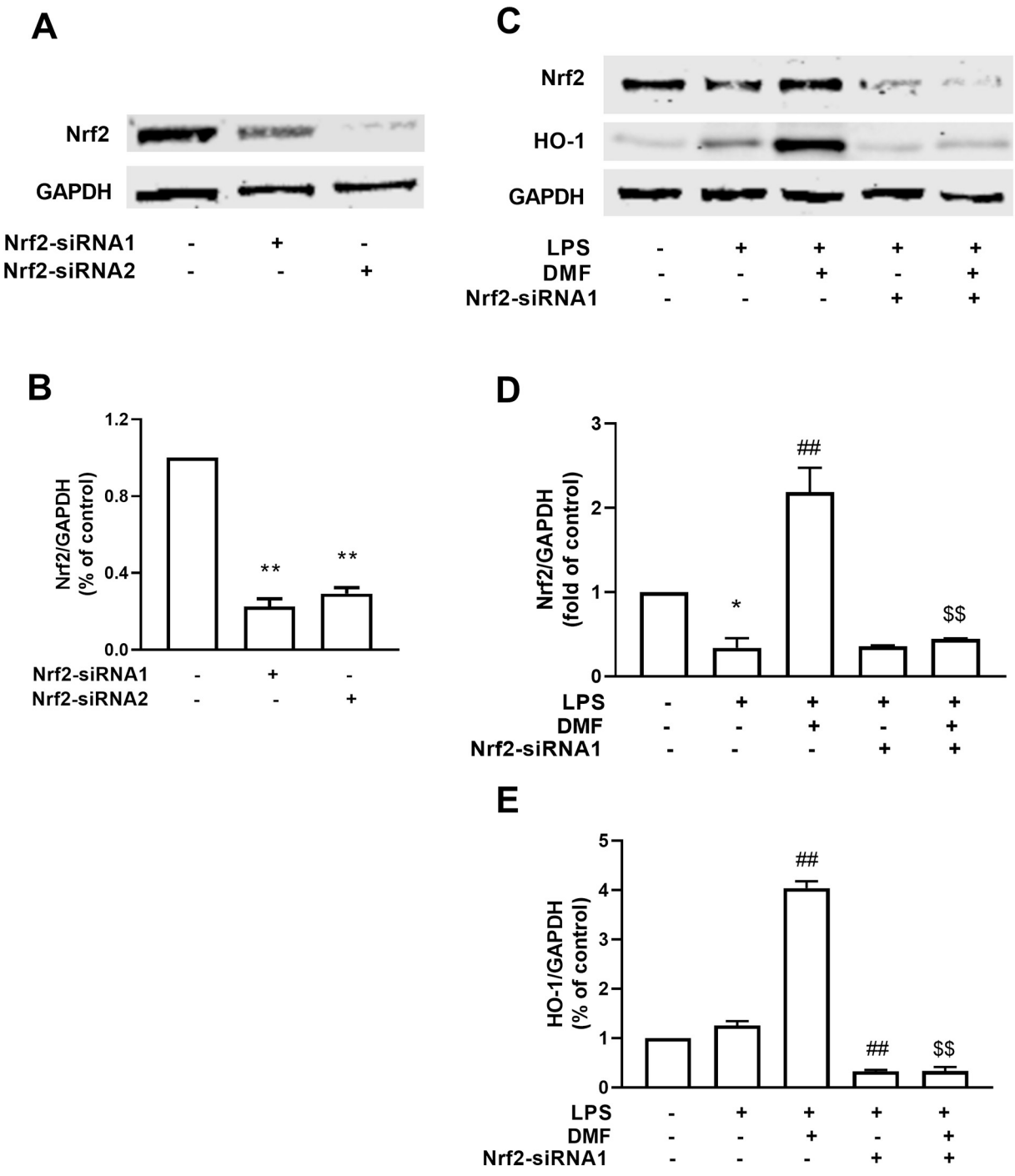

Fig. 4. Effect of Nrf2 on DMF (20 μM)-induced enhancement of HO-1. (A, C) Representative immunoblot obtained with Nrf2, HO-1 and GAPDH antibodies. (B, D, E) Densitometric analysis showing Nrf2 and HO-1 expression. GAPDH was an internal control. Data are mean ± SEM ($n = 3$). $^{*}P < 0.05$, $^{**}P < 0.01$ *vs* control group; $^{\#\#}P < 0.01$ *vs* LPS group. $^{\$\$}P < 0.01$ *vs* LPS + DMF group. (G) Location of Nrf2 protein detected using confocal microscope technique. Scale bars = 20 μm.

2.12. Evaluation of mitochondrial membrane potential

Mitochondrial membrane potential (ΔψM) was evaluated by using JC-1 fluorescent probe. After treatments, cells were stained with 10 μg/ml JC-1 for 20 min at room temperature, and protected from light. The fluorescence signals were recorded using a confocal microscope (Olympus, Tokyo, Japan) at Ex 475 nm/Em 530 nm and 590 nm. A decrease in the ratio of green to red fluorescence indicates decline of mitochondrial membrane potential.

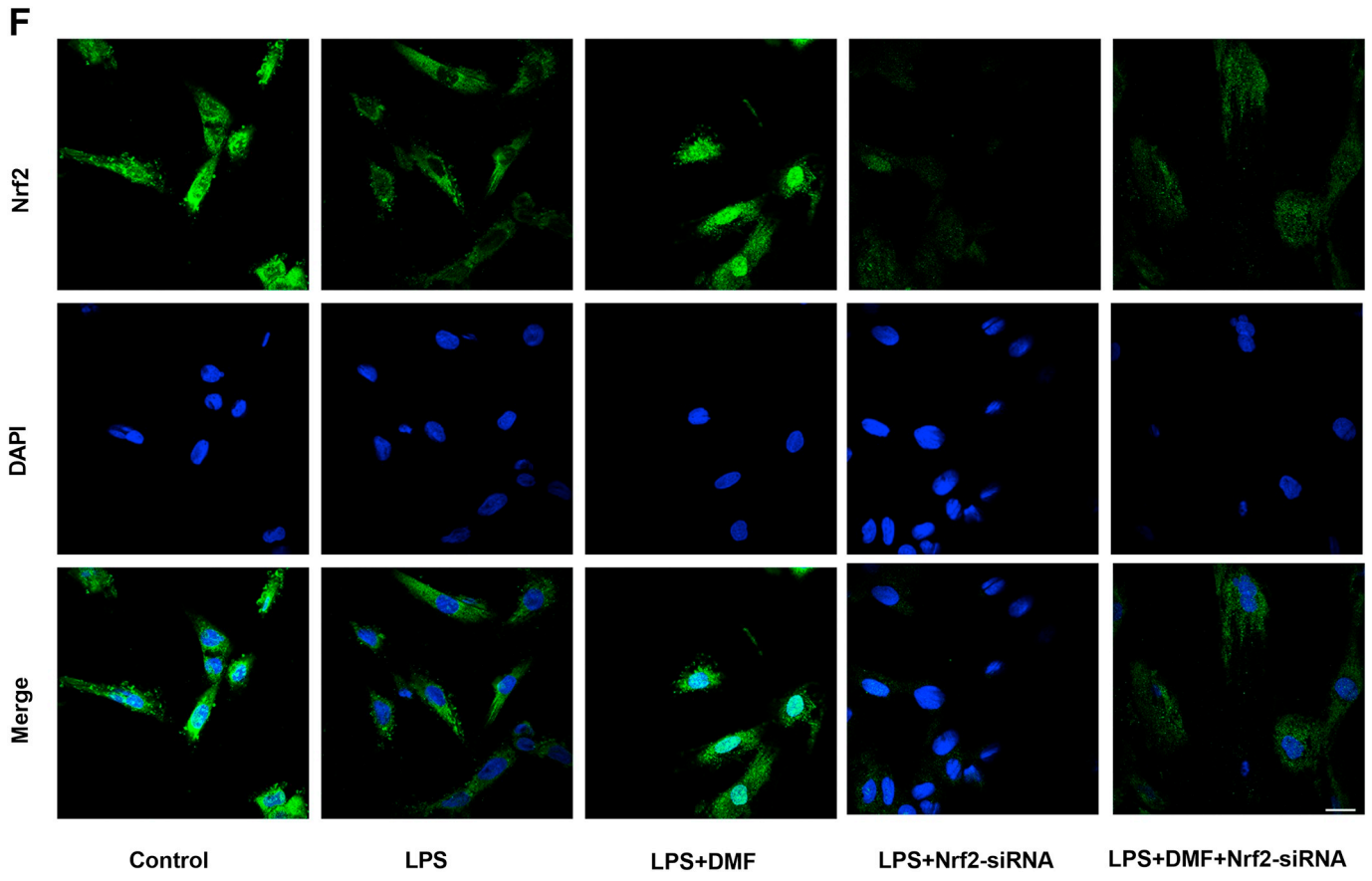

Fig. 4. (*continued*)

2.13. Observation of mitochondrial morphology

Cells were loaded with a mitochondria-specific probe MitoTracker Deep Red (200 nM) for 15 min at 37 °C. Then nuclei was visualized by dying cells with DAPI. Cellular morphology was observed under a confocal microscope. The size and quantity of mitochondria were quantified as Song *et al.* reported [13].

2.14. Mitochondrial respiration assay

Mitochondrial respiration was analyzed by using XF Cell Mito Stress Test Kit (Seahorse Bioscience Inc., Billerica, MA, USA). Cells were incubated in bicarbonate-free DMEM for 30 min. Then oligomycin (1 μM), carbonyl cyanide 4-(trifluoromethoxy) phenylhydrazone (FCCP, 1 μM), and rotenone/antimycin A (0.5 μM) were successively loaded. Oxygen consumption rate (OCR) of basal respiration, spare respiratory capacity, proton leak, and ATP production was recorded by a Seahorse XF96 Analyzer (Seahorse Bioscience, Santa Clara, CA, USA).

2.15. Statistical analysis

Data were expressed as mean ± SEM. Differences between groups were analyzed by one-way ANOVA with Tukey's multiple comparisons test using Prism 8.0.1.

3. Results

3.1. DMF inhibits LPS-induced cell damage in H9c2 cells

DMF alone (10, 20 or 40 μM) has no notable effect on H9c2 cells survival (Fig. 1A). To explore whether DMF can attenuate LPS-induced H9c2 cell injury, cells were pretreated with 0–40 μM DMF for 2 h and then exposed to LPS. The cell viability decreased and LDH activity increased in LPS group (cell viability was 31.6 ± 1.4%, LDH leakage was 19.8 ± 0.3%, $P < 0.01$ *vs* control group, Fig. 1B-C). DMF pretreatment brought a higher cell viability (54.8 ± 0.9%, 86.9 ± 2.0%, 48.2 ± 1.4%, respectively, $P < 0.01$ *vs* LPS group, Fig. 1B) and a lower LDH release than those of LPS group (14.6 ± 0.2%, 12.4 ± 0.2%, 12.5 ± 0.1%, respectively, $P < 0.01$ *vs* LPS group, Fig. 1C). However, 40 μM DMF did not show more benefit effect than 20 μM DMF.

After stimulated by LPS, apoptotic rate of H9c2 cells increased (5.93 ± 0.62%, $P < 0.01$ *vs* control group, Fig. 2). Pretreatment with DMF had an inhibitive effect on LPS-induced apoptosis (3.17 ± 0.31%, 2.57 ± 0.16%, 2.93 ± 0.15%, respectively, $P < 0.01$ *vs* LPS group, Fig. 2).

3.2. DMF induces Nrf2/HO-1 activation in LPS-challenged H9c2 cells

Western blotting results revealed that LPS caused a significant decrease in total Nrf2 protein expression and nuclear Nrf2 level in H9c2

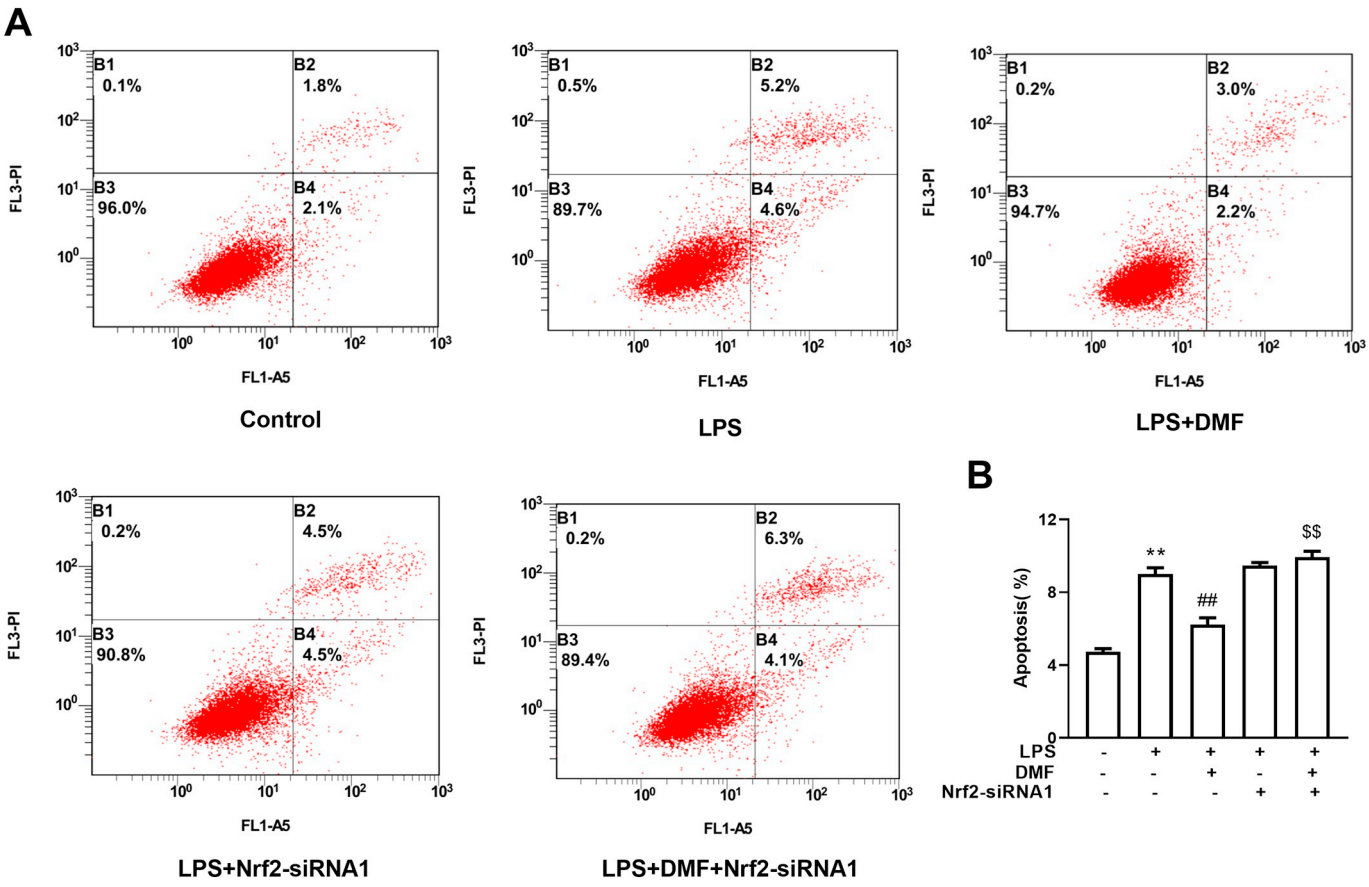

Fig. 5. Effect of Nrf2-siRNA on apoptosis in DMF-treated H9c2 cells. (A) Representative flow cytometry results obtained with A5 and PI. (B) Data analysis showing apoptosis. Data were expressed as mean ± SEM ($n = 6$). $^{**}P < 0.01$ *vs* control group; $^{\#\#}P < 0.01$ *vs* LPS group; $^{\$\$}P < 0.01$ *vs* LPS + DMF group. A5: Annexin V-FITC; PI: propidium iodide.

Table 1
Effect of DMF on LPS-induced oxidative stress and inflammation. (mean ± SEM, $n = 6$).

	Control	LPS	LPS + DMF	LPS + Nrf2-siRNA1	LPS + DMF + Nrf2-siRNA1
Cell viability (% of control)	100.0 ± 0.0	31.0 ± 1.5$_{**}$	87.7 ± 2.2$^{\#\#}$	32.4 ± 0.5	31.6 ± 0.4$^{\$\$}$
LDH leakage (%)	12.8 ± 0.4	25.3 ± 0.7$_{**}$	12.5 ± 0.1$^{\#\#}$	30.5 ± 3.2	37.3 ± 3.3$^{\$\$}$
MDA (μM/mg)	1.97 ± 0.29	3.56 ± 0.14$_{**}$	2.00 ± 0.23$^{\#\#}$	4.04 ± 0.01	4.06 ± 0.01$^{\$\$}$
IL-1β (pg/ml)	86.4 ± 3.1	288.1 ± 26.1$_{**}$	142.9 ± 17.5$^{\#\#}$	283.8 ± 27.2	261.7 ± 23.0$^{\$\$}$
IL-18 (pg/ml)	10.42 ± 2.78	59.73 ± 6.22$_{**}$	28.70 ± 5.30$^{\#\#}$	50.75 ± 8.52	57.00 ± 4.61$^{\$}$
SOD (U/mg)	22.54 ± 1.17	7.76 ± 0.90$_{**}$	24.02 ± 0.96$^{\#\#}$	3.40 ± 0.98$^{\#\#}$	3.43 ± 1.07$^{\$\$}$
GSH-Px (mU/mg)	24.04 ± 2.40	1.32 ± 0.46$_{**}$	15.71 ± 0.39$^{\#\#}$	0.74 ± 0.06$^{\#\#}$	0.92 ± 0.17$^{\$\$}$
GSH (μM/mg)	8.67 ± 0.04	4.64 ± 0.08$_{**}$	7.86 ± 0.39$^{\#\#}$	3.16 ± 0.18$^{\#\#}$	2.82 ± 0.15$^{\$\$}$

** $P < 0.01$ *vs* control group.
$^{\#\#}$ $P < 0.01$ *vs* LPS group.
$^{\$}$ $P < 0.05$.
$^{\$\$}$ $P < 0.01$ *vs* LPS + DMF group.

cells (0.39 ± 0.01 and 0.17 ± 0.01, respectively, $P < 0.05$ *vs* control group, Fig. 3A–E). DMF pretreatment enhanced total and nuclear Nrf2 protein, decreased cytoplasmic Nrf2 protein (Fig. 3A-E, $P < 0.05$). Images from immunofluorescence assay confirmed that DMF pretreatment resulted in an increased translocation of Nrf2 from cytoplasm to nucleus (Fig. 3G). Meanwhile, DMF pretreatment also increased HO-1 expression in LPS-challenged cells (2.52 ± 0.34, 5.29 ± 0.32, 2.28 ± 0.31, respectively, $P < 0.05$ *vs* 1.08 ± 0.09 LPS group, Fig. 3A and F). Thus DMF (20 μM) was chosen to further investigate the mechanism of DMF-induced cardioprotection.

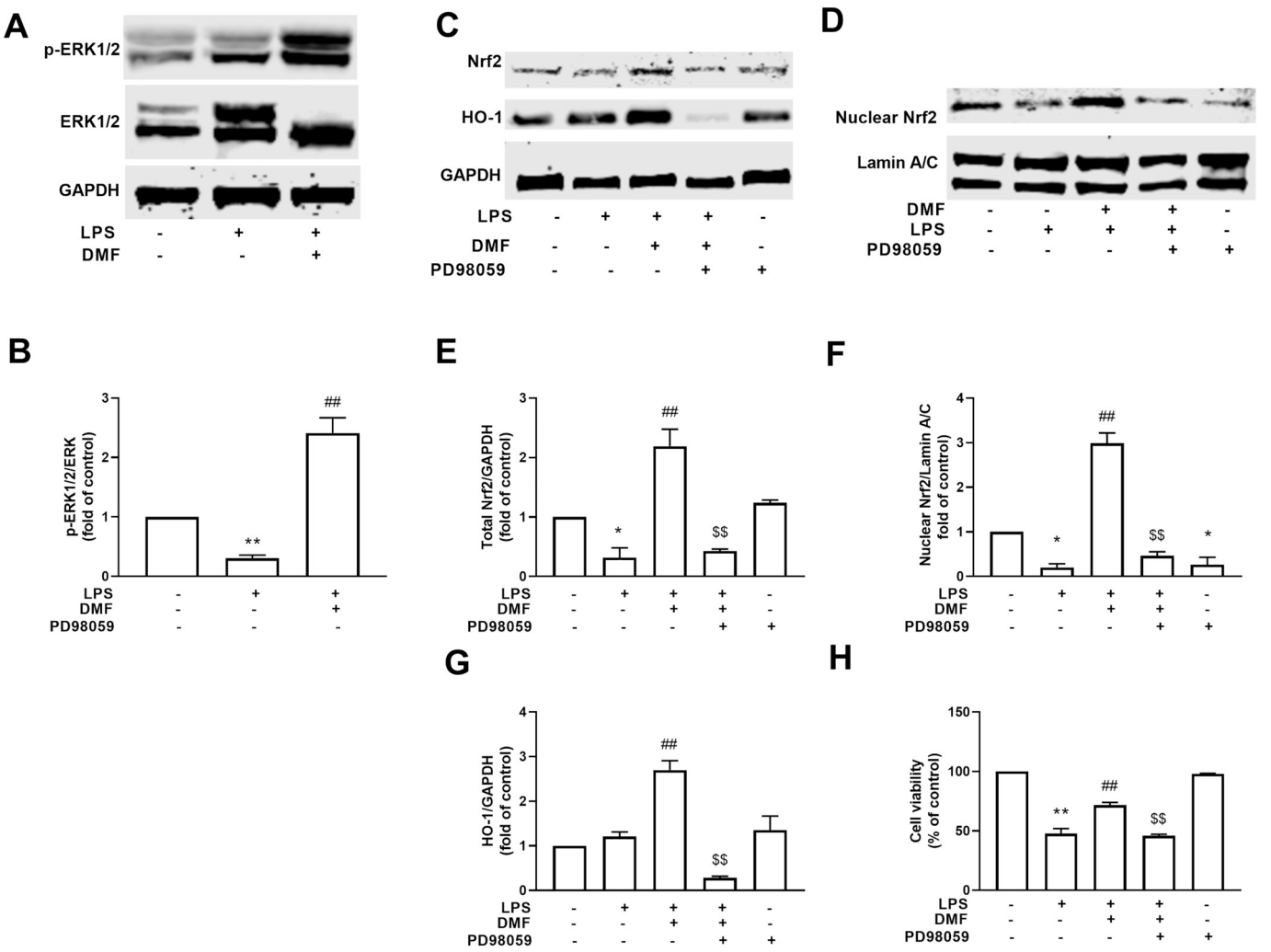

Fig. 6. Effect of ERK1/2 inhibitor PD98059 on DMF-induced Nrf2/HO-1 activation in H9c2 cells. (A, C, D) Representative immunoblot obtained with p-ERK1/2, ERK, Nrf2, HO-1, GAPDH, and Lamin A/C antibodies. (B, E, F, G) Densitometric analysis showing ERK, Nrf2 and HO-1 protein expression. GAPDH and Lamin A/C were served as cytoplasmic or nuclear internal controls, respectively. Data are mean ± SEM ($n = 3$). $^{*}P < 0.05$, $^{**}P < 0.01$ *vs* control group; $^{\#\#}P < 0.01$ *vs* LPS group. $^{\$\$}P < 0.01$ *vs* LPS + DMF group. (H) Cell viability. Data are mean ± SEM ($n = 6$). $^{**}P < 0.01$ *vs* control group; $^{\#\#}P < 0.01$ *vs* LPS group. $^{\$\$}P < 0.01$ *vs* LPS + DMF group. (I) Location of Nrf2 protein detected using confocal microscope technique. Scale bars = 20 μm.

3.3. Effect of Nrf2 on DMF-induced protection against LPS

To further confirm the role of Nrf2 in DMF-induced protection against LPS, cells were transfected with two specific Nrf2-siRNAs. The Western blotting analysis showed that both siRNA1 and siRNA2 had inhibitive effects on the expression of Nrf2 protein (0.22 ± 0.04 and 0.29 ± 0.03, respectively, $P < 0.01$ *vs* control group, Fig. 4A-B). Then Nrf2- siRNA1 was chosen as an Nrf2 inhibitor in further research. After transfected with Nrf2-siRNA1, both Nrf2 and HO-1 expression in DMF-pretreated cells declined (Nrf2 protein was 0.44 ± 0.01, $P < 0.01$ *vs* 2.19 ± 0.29 in LPS + DMF group; HO-1 protein was 0.34 ± 0.08, $P < 0.01$ *vs* 4.04 ± 0.14 in LPS + DMF group, Fig. 4C-E). The changes of Nrf2 expression in different groups were confirmed using immunofluorescence assay (Fig. 4F).

Meanwhile, Nrf2-siRNA2 could also abolish DMF-induced reduction in apoptosis (Fig. 5, $P < 0.01$), inhibit DMF-induced enhancement of survival rate (Table 1, $P < 0.01$). Under the exposure of LPS, LDH leakage, MDA (a marker of oxidative stress) content, inflammatory cytokines (IL-1β and IL-18) concentration were remarkably increased; while SOD and GSH-Px activities, GSH level were significantly decreased, which could be prevented by DMF pretreatment. Nrf2-siRNA2 could inhibit the above beneficial cardioprotection of DMF (Table 1).

3.4. Role of ERK1/2 in DMF-induced Nrf2/HO-1 activation in H9c2 cells

Compared with control group, the ratio of p-ERK1/2/ERK1/2 decreased in LPS group (0.30 ± 0.02, $P < 0.01$ *vs* control group, Fig. 6A–B). DMF pretreatment elevated the ratio of p-ERK1/2/ERK1/2 (2.46 ± 0.17, $P < 0.01$ *vs* LPS group, Fig. 6A–B). Exposed to an ERK1/2 inhibitor PD98059 (40 μM) for 30 min before DMF pretreatment could not only prevent the DMF-induced enhancement of total and nuclear Nrf2 (0.43 ± 0.02 and 0.47 ± 0.09, respectively, $P < 0.01$ *vs*

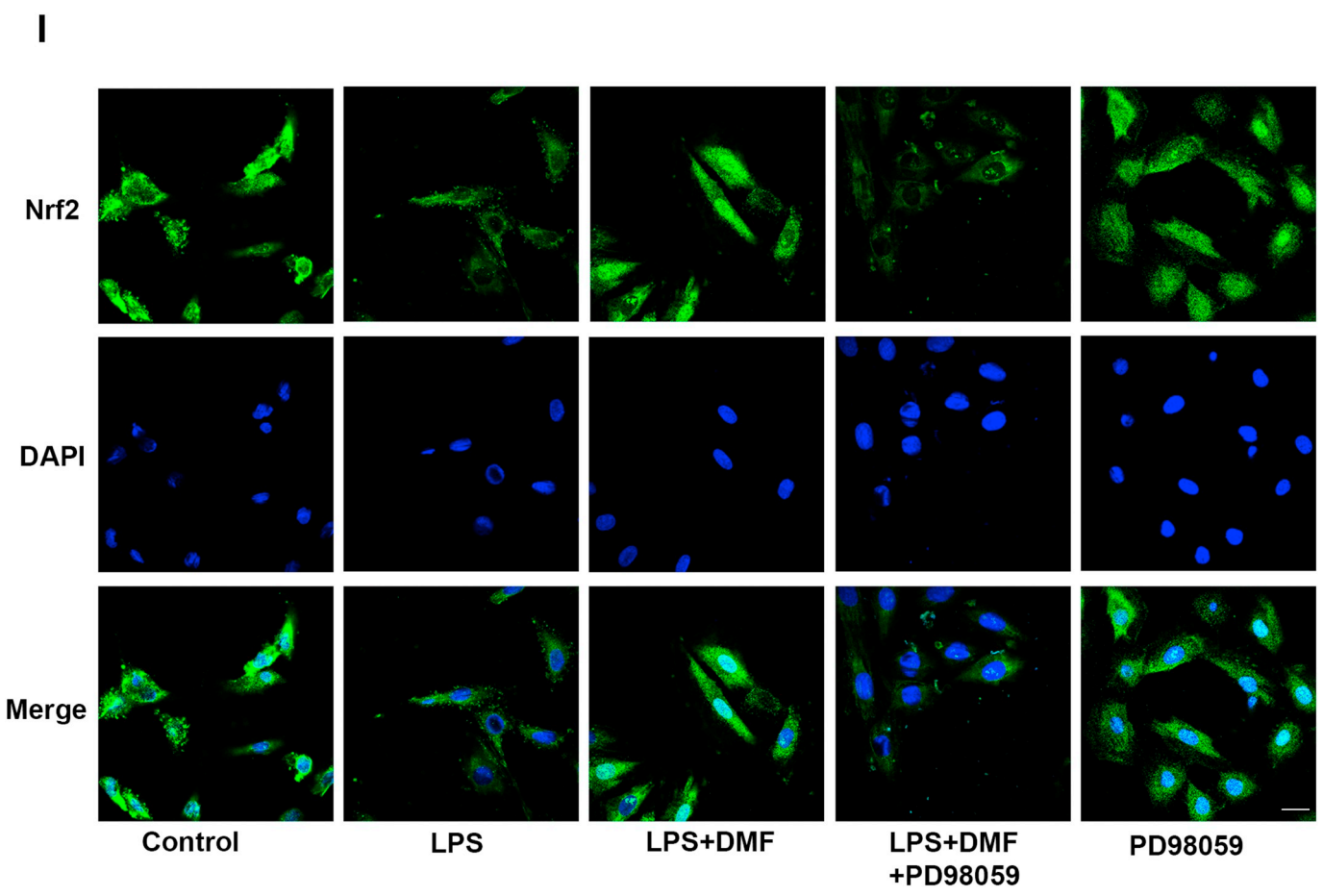

Fig. 6. (*continued*)

LPS + DMF group, Fig. 6C–F), but also inhibit DMF-induced increase in HO-1 expression and cell survival (0.28 ± 0.04 and 45.9 ± 1.3%, respectively, $P < 0.01$ *vs* LPS + DMF group, Fig. 6C, G-H).

3.5. Cardioprotection of DMF against LPS-induced mitochondrial dysfunction and mitochondrial fragmentation

As shown in Fig. 7, LPS could increase the production of mitochondrial superoxide (34.51 ± 2.23, $P < 0.01$ *vs* 12.72 ± 0.56 in control group) and decrease the mitochondrial membrane potential (0.31 ± 0.01, $P < 0.01$ *vs* 5.89 ± 0.57 in control group). Compared with LPS group, DMF pretreatment caused a lower production of mitochondrial superoxide and a higher mitochondrial membrane potential (12.52 ± 0.96 and 5.02 ± 0.27, respectively, $P < 0.01$ *vs* LPS group), which could be abolished by Nrf2-siRNA2 (45.85 ± 3.06 and 0.14 ± 0.01, respectively, $P < 0.01$ *vs* LPS + DMF group).

Mitochondrial morphology was analyzed by using confocal laser microscopy. LPS induced significant reduction of mitochondrial area and remarkable enhancement of mitochondrial quantity (0.26 ± 0.03 μm^2 and 141.30 ± 4.51 per cell respectively, $P < 0.01$ *vs* control group, Fig. 8). Treatment with DMF attenuated LPS-induced mitochondrial fragmentation (mitochondrial area was 1.25 ± 0.13 μm^2 and mitochondrial number per cell was 70.17 ± 4.90, $P < 0.01$ *vs* LPS group, Fig. 8), and Nrf2-siRNA2 could prevent this beneficial effect DMF on mitochondrial morphology (mitochondrial area was 0.13 ± 0.01 μm^2 and mitochondrial number per cell was 141.20 ± 7.39, $P < 0.01$ *vs* LPS + DMF group, Fig. 8).

Results of mitochondrial respiration test showed that exposure to LPS caused a decrease of OCR in the presence of oligomycin, FCCP, and rotenone/antimycin A in H9c2 cells. DMF pretreatment was revealed to significantly improve mitochondrial respiration function by enhancing OCRs of the basal respiration, spare respiratory capacity, proton leak, and ATP production (72.9 ± 4.5, 120.2 ± 12.6, 10.6 ± 0.8, and 62.3 ± 3.7 respectively, $P < 0.01$ *vs* LPS group, Fig. 9). Nrf2-siRNA2 could inhibit the DMF-induced improvement of mitochondrial respiration function (Fig. 9, $P < 0.01$).

4. Discussion

Septic patients with myocardial dysfunction have much higher mortality than those without myocardial dysfunction [4]. In the present study, we used an LPS-induced myocardial dysfunction model to investigate the cardioprotection of DMF.

DMF has been reported to prevent neurological, hepatic, renal, and immunological injury [8,9,14,15]. DMF may also have a protective effect on several cardiovascular disorders. DMF reduces infarct size in rat hearts

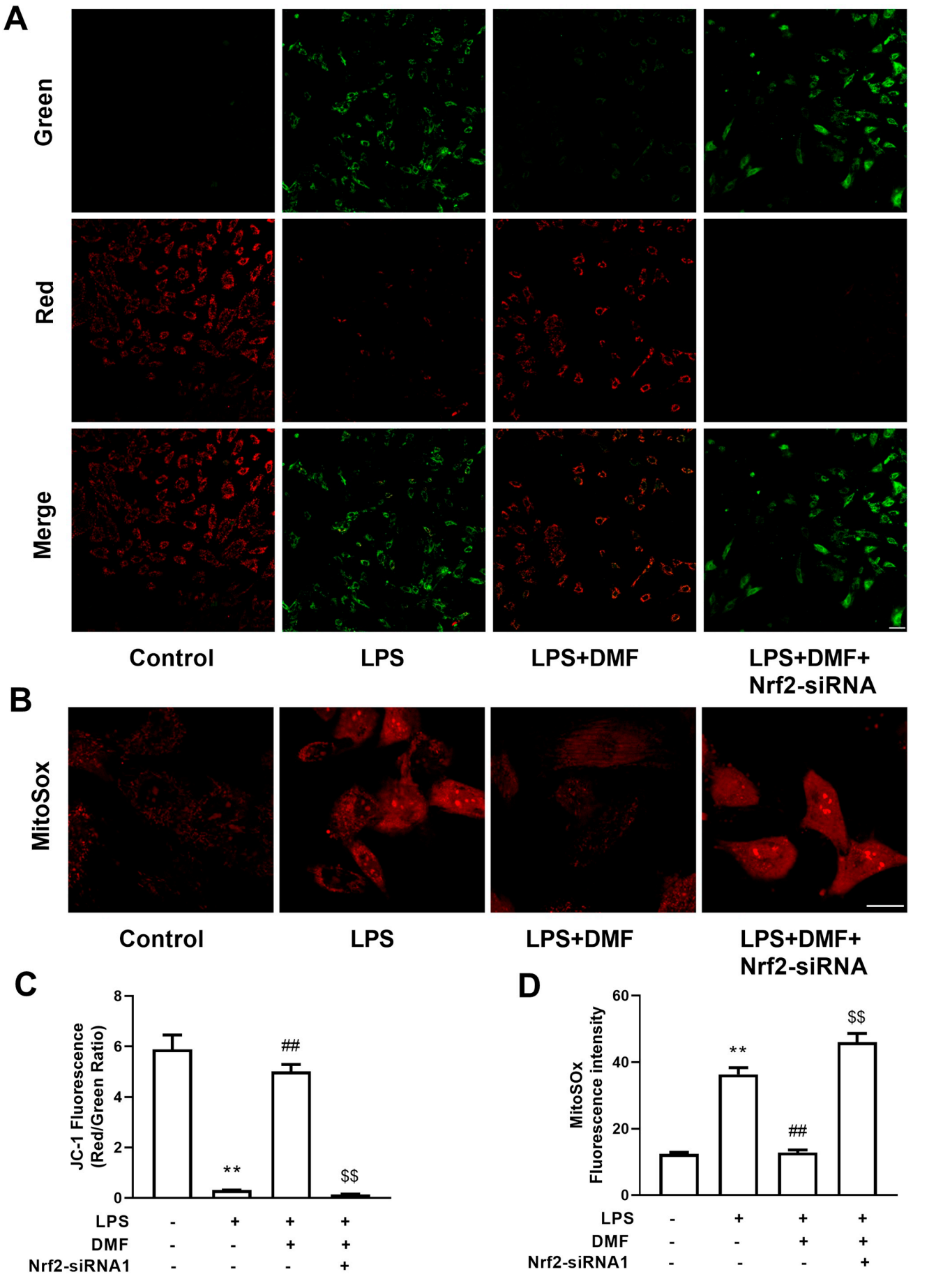

(caption on next page)

Fig. 7. Effect of DMF on LPS-induced changes in mitochondrial membrane potential and superoxide. (A) Representative images of mitochondrial membrane potential detected by JC-1 staining. Scale bars = 40 μm. (B) Representative images of mitochondrial superoxide (Red) detected using MitoSox Red staining. (C–D) Quantitative analysis of mitochondrial membrane potential (C) and mitochondrial superoxide (D). Data are mean ± SEM ($n = 6$). $^{**}P < 0.01$ *vs* control group; $^{\#\#}P < 0.01$ *vs* LPS group; $^{\$\$}P < 0.01$ *vs* LPS + DMF group. (For interpretation of the references to color in this figure legend, the reader is referred to the web version of this article.)

suffered from ischemia-reperfusion [16], ameliorates myosin-induced autoimmune myocarditis in Dark Agouti rats [17], prevents isoproterenol-induced cardiac hypertrophy [10]. Recently, Giustina et al. reported that DMF reduced neutrophil infiltration and alleviated oxidative damage in multiple organs (such as lung, liver, and heart) in CLP-induced septic rats [18]. In the present study, we found that DMF increased cell viability, decreased LDH release and apoptosis in LPS-challenged H9c2 cells, suggesting that DMF may have cardioprotective effect on cardiomyocytes exposed to LPS. However, compared to 20 μM DMF, 40 μM DMF had less effect. This might be because DMF has multiple effects [19] or it can decrease cell viability at a higher concentration [20].

The protective effect of DMF might be contributed to its anti-inflammation and anti-oxidant characteristics [8,9,14,15]. Nrf2 plays a vital role in cardioprotection against oxidative stress [12]. Under inactive state, Nrf2 is mainly retained in cytoplasm by Kelch-like ECH-associated protein 1 (Keap1). Certain pathophysiological and pharmacological stimuli could induce the inactivation of Keap1, lead Nrf2 to be dissociated from Keap1 and translocated into nucleus. After that, Nrf2 induced expression of many antioxidant response element (ARE)-containing genes, which eventually result in activation of the defensive system and maintain the redox homeostasis of cells [21]. DMF could promote nuclear translocation of Nrf2 in HL-1 cells (an embryonic mouse atrial cardiac muscle cell line) [22]. This study demonstrated that DMF induced the increase of total Nrf2 expression and nuclear translocation of Nrf2 in LPS-challenged H9c2 cells, suggesting Nrf2 protein was activated by DMF in H9c2 cardiomyocytes. It has reported that enhancing Nrf2 pathway could protect against sepsis by reducing Toll-like receptor 4 surface trafficking and preventing its downstream signal transducers (Myd88, TRIF) activation [23].

The cardioprotection characteristics of Nrf2 is mainly relevant to the expression of Nrf2-dependent genes and their proteins including HO-1. HO-1 exerts a potential beneficial effect in many cardiovascular disorders through its metabolites biliverdin, Fe^{2+}, and carbon monoxide (CO) [24]. Orally administered HYCO-3 (a compound of CO and DMF) reduced the mRNA levels of IL-1β in brain, liver, lung and heart of septic mice [25]. The present study proved that DMF induced the overexpression of HO-1 protein which could be inhibited by Nrf2-siRNA. Meanwhile, Nrf2-siRNA could not only abolish DMF-induced enhancement of cell viability, but also prevent DMF-induced reduction of LDH release, apoptosis, MDA content, and proinflammatory factors production in LPS-challenged H9c2 cells. The results suggested that Nrf2/HO-1 pathway activation might be involved in the cardioprotection of DMF in cardiac cells.

DMF also exerted sustained neuroprotection in Nrf2-dependent manner [8]. And Nrf2/HO-1 pathway might participate in DMF-induced alleviation of acetaminophen overdose-induce hepatotoxicity [14]. These results were similar with ours in the LPS-challenged cardiomyocytes. In addition to HO-1, Nrf2 regulates other antioxidant and detoxification genes such as SOD, GSH-Px, glutathione reductase, quinone oxidoreductase 1 [26]. The present study showed that DMF did increase SOD and GSH-Px activities in cardiomyocytes exposed to LPS. So cardioprotection of DMF against LPS might be due to Nrf2-dependent mechanism through its antioxidant, anti-inflammation properties. Studies have shown that activation of Nrf2 pathway can inhibit inflammatory response by decreasing of IκB phosphorylation and NF-κB nuclear translocation [27]. The nuclear fraction of Nrf2 is able to bind to the Bcl-2 promoter and activate an anti-apoptotic program [28].

Evidence has shown that phosphorylation of ERK1/2 can inhibit cardiomyocyte apoptosis in the neonatal rat cardiomyocytes [29], increase in heart muscle contractility [30], provide cardioprotection in chronic failing rat heart [31]. Phosphorylation of ERK can enhance the expression of Nrf2 and its downstream genes to protect skin cells against oxidative stress [32]. Xu et al. demonstrated that phosphorylated ERK triggered nuclear translocation of Nrf2 by phosphorylation of Nrf2 Ser40 [33]. Here, we found that DMF increased the phosphorylation of ERK1/2. Moreover, a specific inhibitor of ERK1/2 prevented DMF-induced Nrf2 overexpression and nuclear translocation, inhibited DMF-induced enhancement of HO-1 protein expression and cell viability. These results indicated that ERK1/2 might be the upstream signal molecular involved in DMF-induced activation of Nrf2 in LPS-challenged cardiomyocytes.

Binding of LPS with Toll-like receptor is proven to provoke the production of mitochondrial ROS through mtDNA damage, and result in cardiac inflammation and mitochondrial fragment [34,35]. Furthermore, morphologically abnormal mitochondria induced by oxidative stress could in turn accelerate ROS production in mitochondria [36]. Decrease in mitochondrial membrane potential not only leads to depletion of cellular ATP level, but also enhances ROS production [37]. A recent report has shown that DMF could stimulate mitochondrial biogenesis, increases mitochondrial complex expression in human fibroblast cells [38]. Our present study showed that DMF ameliorated LPS-induced superoxide overproduction and mitochondrial fragment, increased mitochondrial membrane potential and mitochondrial OCRs, which could be abolished by Nrf2–siRNA. The results indicated that the cardioprotective mechanism of DMF may be related to prevention of ROS production, which in turn maintains mitochondrial morphology, promotes mitochondrial respiration function, and protects against LPS-induced injury.

5. Conclusion

In conclusion, DMF could protect H9c2 cells from LPS-induced damage. ERK1/2-dependent activation of Nrf2/HO-1 pathway is responsible for DMF-induced cardioprotection *via* reduction of oxidative stress, improvement of mitochondrial morphology and energy metabolism (Fig. 10). The findings indicate that DMF might act as a potential medicine for patients suffered from septic cardiomyopathy through improvement of cardiac mitochondrial function.

Declaration of competing interest

There is no conflict of interest.

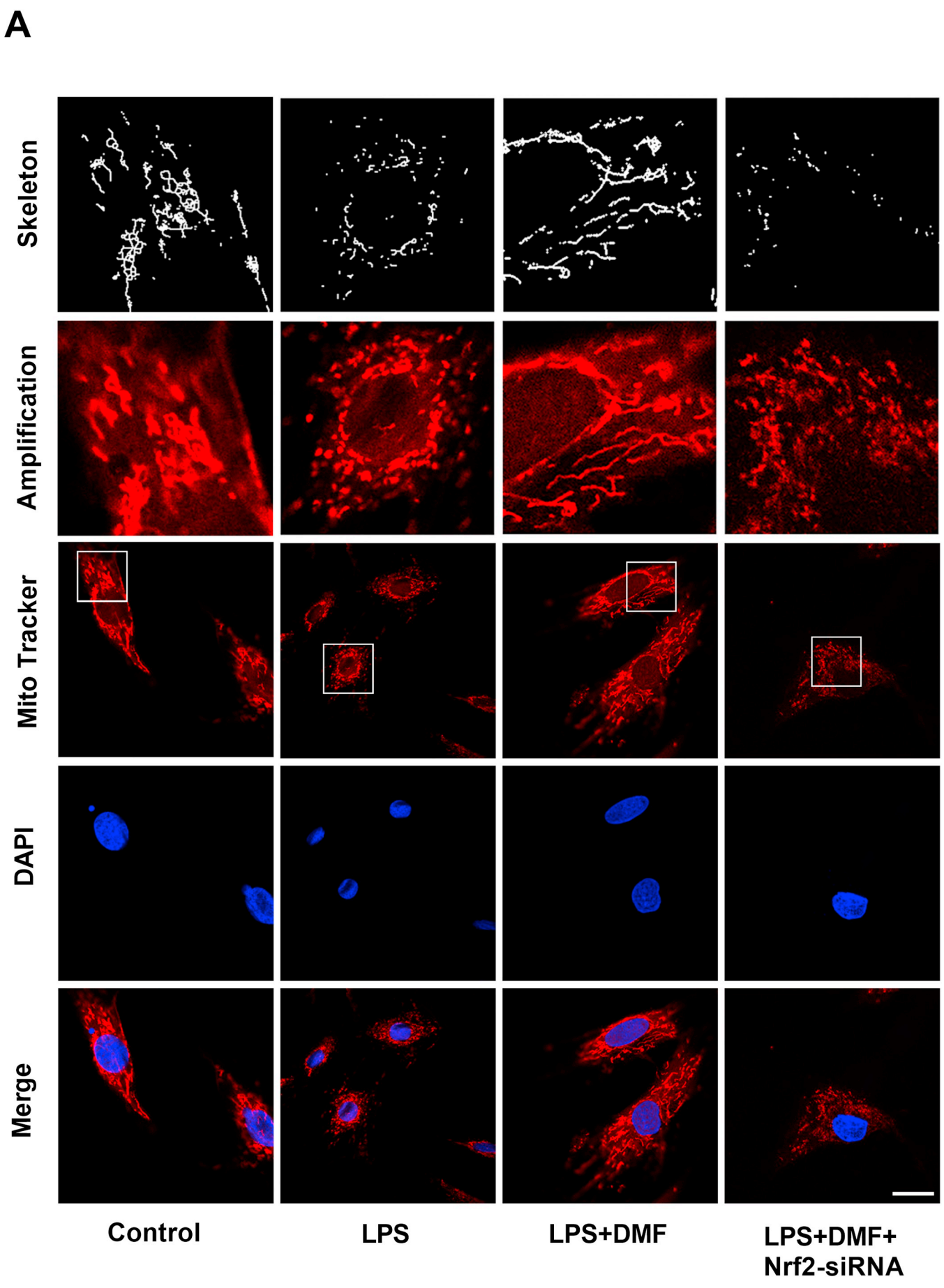

(caption on next page)

Fig. 8. Effect of DMF on LPS-induced changes in mitochondria morphology. (A) Representative images of mitochondrial morphology observed under confocal laser scanning microscope. Mitochondria (red) were indicated by MitoTracker Deep Red. Scale bars = 20 μm. (B–C) Data analyses of mitochondrial quantity (B) and mitochondrial area (C). Data are mean ± SEM ($n = 6$). $^{**}P < 0.01$ *vs* control group; $^{\#\#}P < 0.01$ *vs* LPS group; $^{\$\$}P < 0.01$ *vs* LPS + DMF group. (For interpretation of the references to colour in this figure legend, the reader is referred to the web version of this article.)

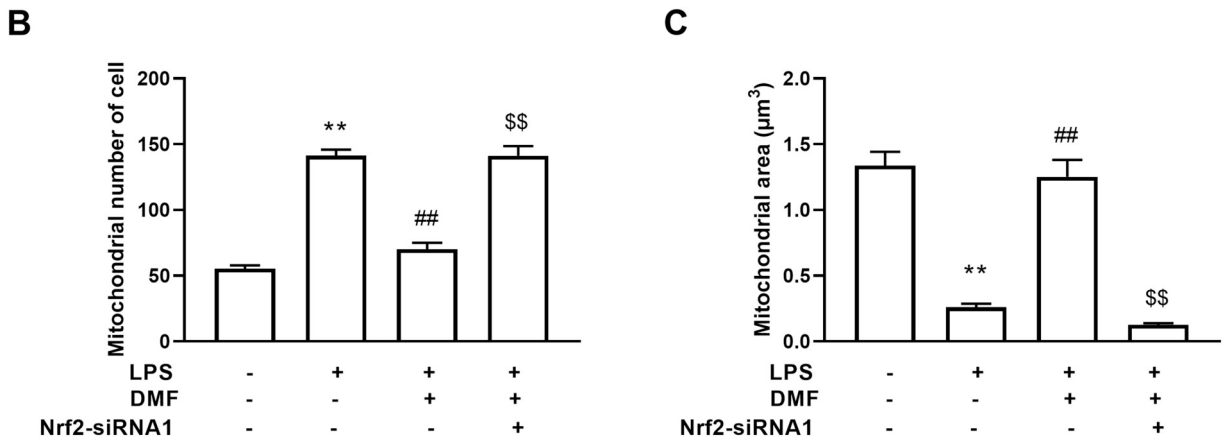

Fig. 8. (*continued*)

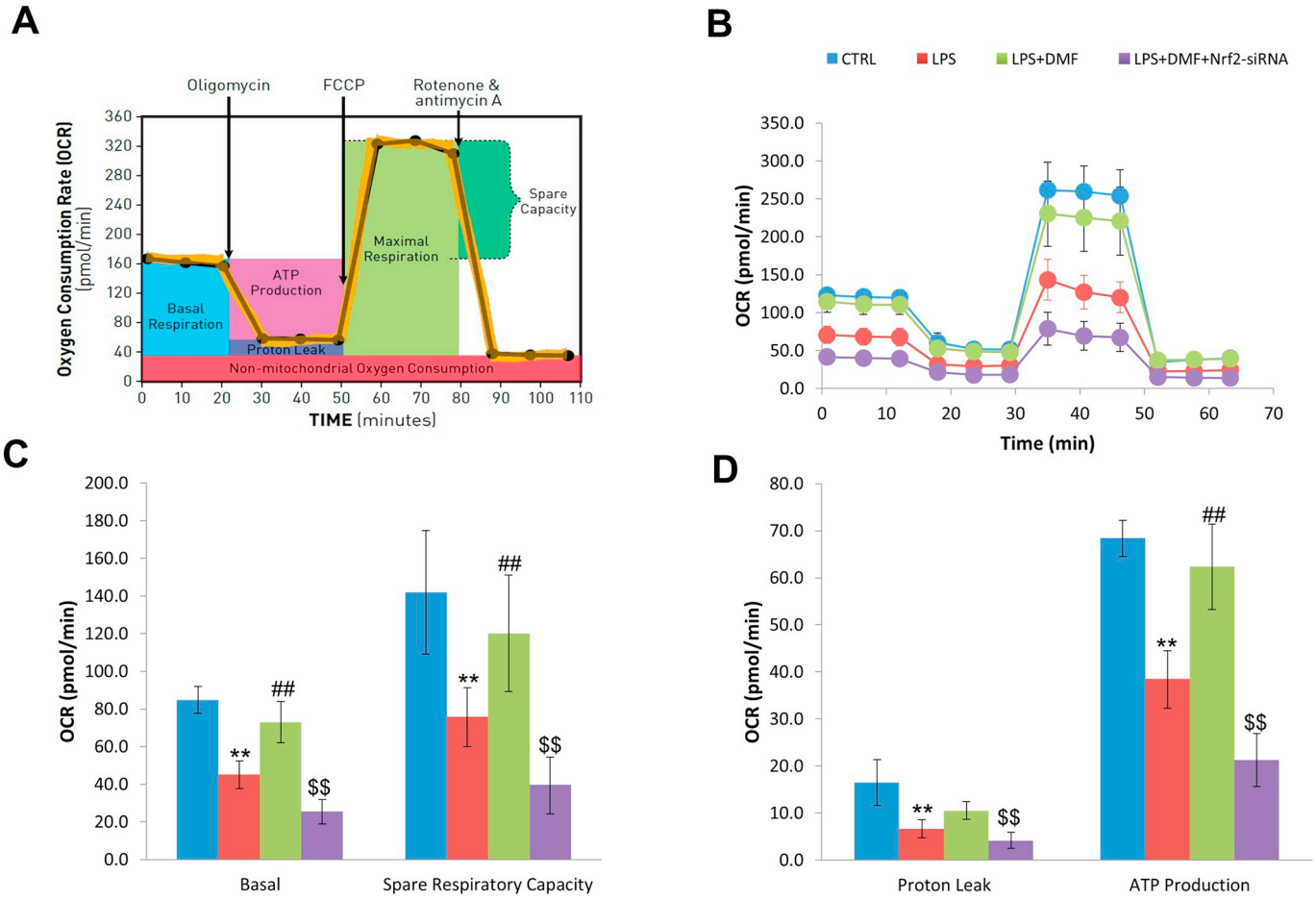

Fig. 9. Effect of DMF on LPS-induced mitochondrial respiration dysfunction. (A) Schematic of mitochondrial respiration. Basal respiration was acquired after subtraction of non-mitochondrial respiration. ATP production and proton leak were acquired with the addition of the oligomycin. Maximal respiration was calculated with the addition of FCCP. Spare capacity was measured by subtracting basal respiration from maximal respiration. (B) Representative images of oxygen consumption rate (OCR) curve; (C) Quantitative analysis of basal respiration and spare respiratory capacity; (D) Quantitative analysis of proton leak and ATP production. Data are mean ± SEM ($n = 6$). $^{**}P < 0.01$ *vs* control group; $^{\#\#}P < 0.01$ *vs* LPS group; $^{\$\$}P < 0.01$ *vs* LPS + DMF group.

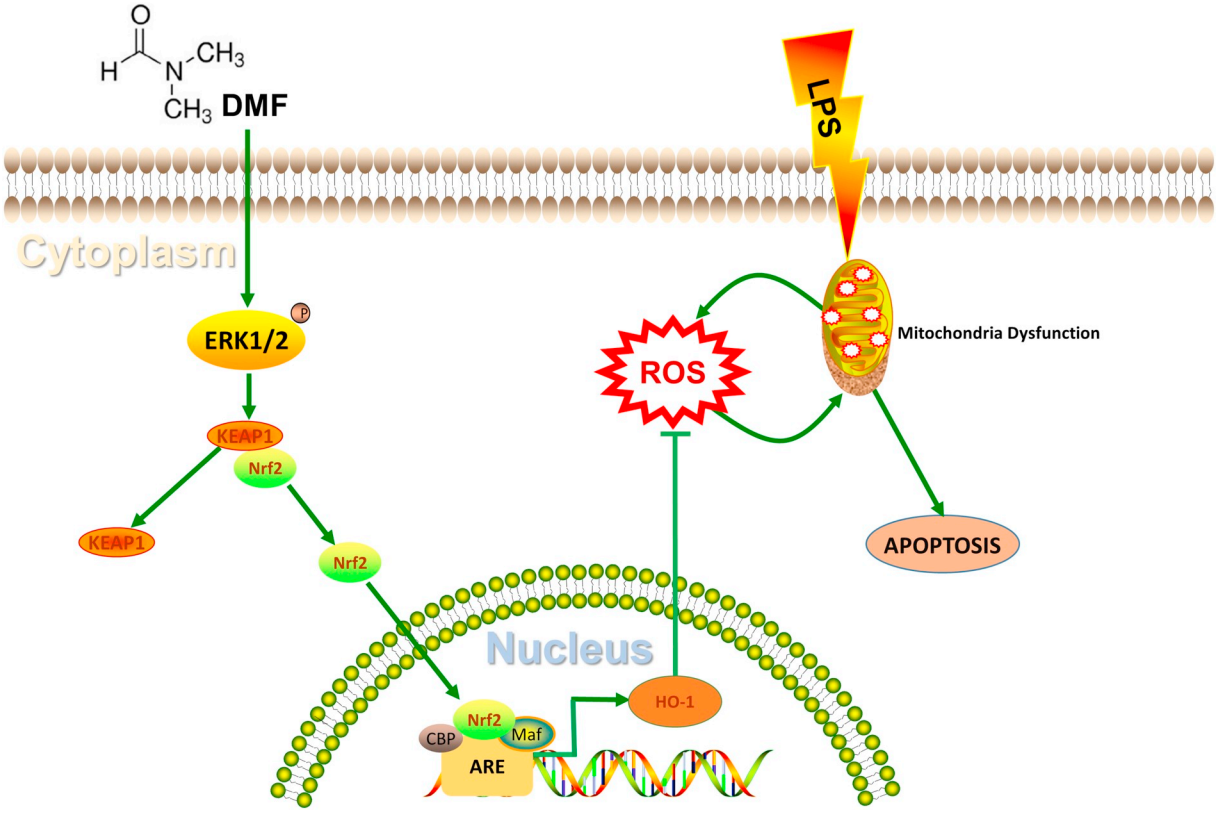

Fig. 10. A schematic diagram of protection of DMF against LPS-induced cardiomyocyte injury by activating Nrf2/HO-1 pathway.

Acknowledgements

This work was supported by the National Natural Science Foundation of China (grant number: 81871541 and 81471837), and Zhejiang Provincial Medical and Health Science Technology Program (grant number: 2019KY366).

References

[1] C. Fleischmann, A. Scherag, N.K. Adhikari, C.S. Hartog, T. Tsaganos, P. Schlattmann, et al., Assessment of global incidence and mortality of hospital-treated sepsis. Current estimates and limitations, Am. J. Respir. Crit. Care Med. 193 (2016) 259–272.
[2] S.L. Zanotti-Cavazzoni, S.M. Hollenberg, Cardiac dysfunction in severe sepsis and septic shock, Curr. Opin. Crit. Care 15 (2009) 392–397.
[3] M.W. Merx, C. Weber, Sepsis and the heart, Circulation 116 (2007) 793–802.
[4] S. Alvarez, T. Vico, V. Vanasco, Cardiac dysfunction, mitochondrial architecture, energy production, and inflammatory pathways: interrelated aspects in endotoxemia and sepsis, Int. J. Biochem. Cell Biol. 81 (2016) 307–314.
[5] Q.S. Zang, H. Sadek, D.L. Maass, B. Martinez, L. Ma, J.A. Kilgore, et al., Specific inhibition of mitochondrial oxidative stress suppresses inflammation and improves cardiac function in a rat pneumonia-related sepsis model, Am. J. Physiol. Heart Circ. Physiol. 302 (2012) H1847–H1859.
[6] D. Werdenberg, R. Joshi, S. Wolffram, H.P. Merkle, P. Langguth, Presystemic metabolism and intestinal absorption of antipsoriatic fumaric acid esters, Biopharm. Drug Dispos. 24 (2003) 259–273.
[7] A. Zarrouk, T. Nury, E.M. Karym, A. Vejux, R. Sghaier, C. Gondcaille, et al., Attenuation of 7-ketocholesterol-induced overproduction of reactive oxygen species, apoptosis, and autophagy by dimethyl fumarate on 158N murine oligodendrocytes, J. Steroid Biochem. Mol. Biol. 169 (2017) 29–38.
[8] L. Liu, M.K. Vollmer, A.S. Ahmad, V.M. Fernandez, H. Kim, S. Dore, Pretreatment with Korean red ginseng or dimethyl fumarate attenuates reactive gliosis and confers sustained neuroprotection against cerebral hypoxic-ischemic damage by an Nrf2-dependent mechanism, Free Radic. Biol. Med. 131 (2019) 98–114.
[9] Y. Yao, W. Miao, Z. Liu, W. Han, K. Shi, Y. Shen, et al., Dimethyl fumarate and monomethyl fumarate promote post-ischemic recovery in mice, Transl. Stroke Res. 7 (2016) 535–547.
[10] A.A. Ahmed, A.A.E. Ahmed, E.M. El Morsy, S. Nofal, Dimethyl fumarate interferes with MyD88-dependent toll-like receptor signalling pathway in isoproterenol-induced cardiac hypertrophy model, J. Pharm. Pharmacol. 70 (2018) 1521–1530.
[11] T.Y. Wu, T.O. Khor, J.H. Lee, K.L. Cheung, L. Shu, C. Chen, et al., Pharmacogenetics, pharmacogenomics and epigenetics of Nrf2-regulated xenobiotic-metabolizing enzymes and transporters by dietary phytochemical and cancer chemoprevention, Curr. Drug Metab. 14 (2013) 688–694.
[12] Q.M. Chen, A.J. Maltagliati, Nrf2 at the heart of oxidative stress and cardiac protection, Physiol. Genomics 50 (2018) 77–97.
[13] W. Song, B. Bossy, O.J. Martin, A. Hicks, S. Lubitz, A.B. Knott, et al., Assessing mitochondrial morphology and dynamics using fluorescence wide-field microscopy and 3D image processing, Methods 46 (2008) 295–303.
[14] R.S. Abdelrahman, N. Abdel-Rahman, Dimethyl fumarate ameliorates acetaminophen-induced hepatic injury in mice dependent of Nrf-2/HO-1 pathway, Life Sci. 217 (2019) 251–260.
[15] A. Sasaki, N. Koike, T. Murakami, K. Suzuki, Dimethyl fumarate ameliorates cisplatin-induced renal tubulointerstitial lesions, J. Toxicol. Pathol. 32 (2019) 79–89.
[16] S. Meili-Butz, T. Niermann, E. Fasler-Kan, V. Barbosa, N. Butz, D. John, et al., Dimethyl fumarate, a small molecule drug for psoriasis, inhibits nuclear factor-kappaB and reduces myocardial infarct size in rats, Eur. J. Pharmacol. 586 (2008) 251–258.
[17] M. Milenkovic, N. Arsenovic-Ranin, D. Vucicevic, B. Bufan, I. Jancic, Z. Stojic-Vukanic, Beneficial effects of dimethyl fumarate on experimental autoimmune myocarditis, Arch. Med. Res. 39 (2008) 639–646.
[18] A.D. Giustina, S. Bonfante, G.F. Zarbato, L.G. Danielski, K. Mathias, A.N. de Oliveira Jr.et al., Dimethyl fumarate modulates oxidative stress and inflammation in organs after sepsis in rats, Inflammation 41 (2018) 315–327.
[19] N.E.B. Saidu, N. Kavian, K. Leroy, C. Jacob, C. Nicco, F. Batteux, et al., Dimethyl fumarate, a two-edged drug: current status and future directions, Med. Res. Rev. 39 (2019) 1923–1952.
[20] X. Xie, Y. Zhao, C.Y. Ma, X.M. Xu, Y.Q. Zhang, C.G. Wang, et al., Dimethyl fumarate induces necroptosis in colon cancer cells through GSH depletion/ROS increase/MAPKs activation pathway, Br. J. Pharmacol. 172 (2015) 3929–3943.
[21] M.C. Lu, J.A. Ji, Z.Y. Jiang, Q.D. You, The Keap1-Nrf2-ARE pathway as a potential preventive and therapeutic target: an update, Med. Res. Rev. 36 (2016) 924–963.
[22] H. Ashrafian, G. Czibik, M. Bellahcene, D. Aksentijevic, A.C. Smith, S.J. Mitchell, et al., Fumarate is cardioprotective via activation of the Nrf2 antioxidant pathway, Cell Metab. 15 (2012) 361–371.
[23] X. Kong, R. Thimmulappa, F. Craciun, C. Harvey, A. Singh, P. Kombairaju, et al., Enhancing Nrf2 pathway by disruption of Keap1 in myeloid leukocytes protects against sepsis, Am. J. Respir. Crit. Care Med. 184 (2011) 928–938.
[24] M.L. Wu, Y.C. Ho, C.Y. Lin, S.F. Yet, Heme oxygenase-1 in inflammation and cardiovascular disease, Am J Cardiovasc Dis 1 (2011) 150–158.
[25] R. Motterlini, A. Nikam, S. Manin, A. Ollivier, J.L. Wilson, S. Djouadi, et al., HYCO-3, a dual CO-releaser/Nrf2 activator, reduces tissue inflammation in mice challenged with lipopolysaccharide, Redox Biol. 20 (2019) 334–348.

[26] L. Zhao, X. Tao, Y. Qi, L. Xu, L. Yin, J. Peng, Protective effect of dioscin against doxorubicin-induced cardiotoxicity via adjusting microRNA-140-5p-mediated myocardial oxidative stress, Redox Biol. 16 (2018) 189–198.
[27] T. Qin, R. Du, F. Huang, S. Yin, J. Yang, S. Qin, et al., Sinomenine activation of Nrf2 signaling prevents hyperactive inflammation and kidney injury in a mouse model of obstructive nephropathy, Free Radic. Biol. Med. 92 (2016) 90–99.
[28] P. Gupta, S. Choudhury, S. Ghosh, S. Mukherjee, O. Chowdhury, A. Sain, et al., Dietary pomegranate supplement alleviates murine pancreatitis by modulating Nrf2-p21 interaction and controlling apoptosis to survival switch, J. Nutr. Biochem. 66 (2019) 17–28.
[29] D.M. Valks, S.A. Cook, F.H. Pham, P.R. Morrison, A. Clerk, P.H. Sugden, Phenylephrine promotes phosphorylation of Bad in cardiac myocytes through the extracellular signal-regulated kinases 1/2 and protein kinase A, J. Mol. Cell. Cardiol. 34 (2002) 749–763.
[30] N. Buzaglo, H. Rosen, H.C. Ben Ami, A. Inbal, D. Lichtstein, Essential opposite roles of ERK and Akt signaling in cardiac steroid-induced increase in heart contractility, J. Pharmacol. Exp. Ther. 357 (2016) 345–356.
[31] S.Y. Jin, J. Huang, H.J. Zhu, H. Wu, S.J. Xu, M.G. Irwin, et al., Remifentanil preconditioning confers cardioprotection via c-Jun NH2-terminal kinases and extracellular signal regulated kinases pathways in ex-vivo failing rat heart, Eur. J. Pharmacol. 828 (2018) 1–8.
[32] Y.S. Ryu, P. Fernando, K.A. Kang, M.J. Piao, A.X. Zhen, H.K. Kang, et al., Marine compound 3-bromo-4,5-dihydroxybenzaldehyde protects skin cells against oxidative damage via the Nrf2/HO-1 pathway, Mar Drugs 17 (2019) e234.
[33] L.L. Xu, T. Liu, L. Wang, L. Li, Y.F. Wu, C.C. Li, et al., 3-(1H-benzo[d]imidazol-6-yl)-5-(4-fluorophenyl)-1,2,4-oxadiazole (DDO7232), a novel potent Nrf2/ARE inducer, ameliorates DSS-induced murine colitis and protects NCM460 cells against oxidative stress via ERK1/2 phosphorylation, Oxidative Med. Cell. Longev. 2018 (2018) (3271617).
[34] X. Yao, D. Carlson, Y. Sun, L. Ma, S.E. Wolf, J.P. Minei, et al., Mitochondrial ROS induces cardiac inflammation via a pathway through mtDNA damage in a pneumonia-related sepsis model, PLoS One 10 (2015) e0139416.
[35] B. Wu, J. Li, H. Ni, X. Zhuang, Z. Qi, Q. Chen, et al., TLR4 activation promotes the progression of experimental autoimmune myocarditis to dilated cardiomyopathy by inducing mitochondrial dynamic imbalance, Oxidative Med. Cell. Longev. 2018 (2018) 3181278.
[36] H. Tang, K. Inoki, S.V. Brooks, H. Okazawa, M. Lee, J. Wang, et al., mTORC1 underlies age-related muscle fiber damage and loss by inducing oxidative stress and catabolism, Aging Cell 18 (2019) e12943.
[37] A. Roy, A. Ganguly, S. BoseDasgupta, B.B. Das, C. Pal, P. Jaisankar, et al., Mitochondria-dependent reactive oxygen species-mediated programmed cell death induced by 3,3′-diindolylmethane through inhibition of F0F1-ATP synthase in unicellular protozoan parasite Leishmania donovani, Mol. Pharmacol. 74 (2008) 1292–1307.
[38] G. Hayashi, M. Jasoliya, S. Sahdeo, F. Sacca, C. Pane, A. Filla, et al., Dimethyl fumarate mediates Nrf2-dependent mitochondrial biogenesis in mice and humans, Hum. Mol. Genet. 26 (2017) 2864–2873.